Mineralogy and Petrology (2002) 75: 1–21

Mineralogy and Petrology

Geochemistry of metasomatised spinel peridotite xenoliths from the Dariganga Plateau, South-eastern Mongolia

V. A. Kononova[1], **G. Kurat**[2], **A. Embey-Isztin**[3], **V. A. Pervov**[1], **C. Koeberl**[4], and **F. Brandstätter**[2]

[1] Institute of Geology of Ore Deposits, Petrography, Mineralogy, and Geochemistry (IGEM), Russian Academy of Sciences, Moscow, Russia
[2] Naturhistorisches Museum, Vienna, Austria
[3] Temeszettudomanyi Muzeum, Budapest, Hungary
[4] Institut für Geochemie, Universität Wien, Vienna, Austria

With 5 Figures

Received May 28, 1999;
revised version accepted February 24, 2001

Summary

One fresh (green), one altered (black) and one composite (green/black) peridotite xenolith from the Neogene-Quaternary basalts of the Dariganga Plateau, SE Mongolia, were studied by electron microprobe, X-ray fluorescence, wet chemical and instrumental neutron activation analysis.

The history of the upper mantle underneath the Dariganga Plateau has been complex and is characterised by elemental depletions and enrichments processes. The rocks investigated appear to have been processed in several steps, have been moderately depleted (relative to the primitive upper mantle composition) in incompatible elements and subsequently metasomatically enriched in alkalis, Fe, Ca, LREE, Th and U. As a result, most peridotites are moderately depleted in Si, Cr, Ti, HREE and Hf, are slightly enriched in LREE and have elevated Th and U abundances. The minerals in all rocks are out of chemical equilibrium. In the green peridotites disequilibrium is modest but it is severe in the blackened lherzolites. The latter have experienced strong Fe metasomatism accompanied by strong oxidation. As a result, Mg-rich olivines formed by oxidation and precipitation of Fe oxides in the primary olivines (blackening) and Fe-rich olivines formed in the Fe metasomatic event. The latter could only have taken place after the oxidising event, otherwise the Fe-rich olivines would also have been affected by it.

Three of the four rocks show negative anomalies (relative to the Ce abundance) of Hf and Ti, one is enriched in these elements, which is considered an indication of the

action of carbonatitic melts/fluids in the upper mantle. Enrichment of U over Th in some of our samples seems also to indicate the presence of water in the fluid phase, however, the lack of (OH)-bearing minerals in the Dariganga xenoliths suggests a low activity of water in these fluids. The latest of the metasomatic events probably took place shortly before entrapment of the rocks by the basaltic lava that carried them to the earth's surface.

The composite sample consisting of a green harzburgite and a black lherzolite suggests that blackening took place at the original location of the rock rather than in the basaltic tuff because the latter should have altered the whole xenolith. It also demonstrates that metasomatic processes in the upper mantle can be confined to rather restricted locations with sharp boundaries towards the wall rocks. Blackening as well as the metasomatic events apparently took place because of a better permeability in one part of the rock as compared to the other, probably the result of tectonisation.

Introduction

The Neogene-Quaternary volcanic region of the Dariganga Plateau, south-eastern Mongolia, occupies an intermediary position between the Lake Baikal-Central Mongolian graben system and the subduction-related Sikhote-Alin Ridge in the Far East (Fig. 1). Thus, it provides an important link between the volcanic fields and their xenolith occurrences in the intercontinental Baikal rift zone and those of the Pacific margin of Asia. The alkali basalt fields associated with the Baikal rift (Vitim, Bartoi, Khamar-Daban and Taryat, Fig. 1) are located in an area marked by a geophysically anomalous mantle with the presence of a low-velocity asthenospheric bulge along the rift axis. The uplifted Dariganga Plateau is outside of this well-defined intercontinental rift zone. Below this particular region, the lithosphere is thick and the substantial volcanism probably indicates the presence of a hot spot (*Zorin*, 1981; *Ionov* et al., 1992). However, both rifting in the Baikal-Central Mongolian graben and doming and uplifting further south in the Khangai Rise and Dariganga Plateau are thought to be the result of the collision between the Indian and Eurasian plates initiated in the Eocene (*Tapponnier* and *Molnár*, 1979; *Zonenshain* and *Savostin*, 1981).

The Dariganga Plateau straddles the border between Mongolia and China and is the largest Cenozoic lava field in central and eastern Asia (Fig. 1). The basement is mainly composed of Late Proterozoic and Precambrian rocks, although Mesozoic granites are also common in the region. The volcanic activity started around 14 Ma ago and ended as late as 1.6 Ma, but the majority of rocks is younger than 5 Ma (*Kononova* et al., 1988; *Genshaft* and *Saltykovsky*, 1990). The lowest part of the plateau is composed of Miocene lava flows, whereas Quaternary lava flows and pyroclastics form numerous volcanic cones. The lavas show alkaline affinities, being mostly olivine tephrites and olivine basalts. According to *Kononova* et al. (1987), the Miocene basalts are only mildly undersaturated, with a normative nepheline content ranging from 1.3 to 5.8 wt%, whereas the younger Pleistocene volcanic rocks are more strongly undersaturated (3.4–10.9 % normative *ne*). None of the basalts is primitive in composition and the relatively low mg-numbers (100 $Mg/(Mg + Fe^{2+})$), between 55 and 67, indicate that the lavas are differentiated.

Ultramafic xenoliths (spinel and garnet lherzolite, websterite, clinopyroxenite, amphibole-bearing garnet pyroxenite), as well as megacrysts of Al-clinopyroxene,

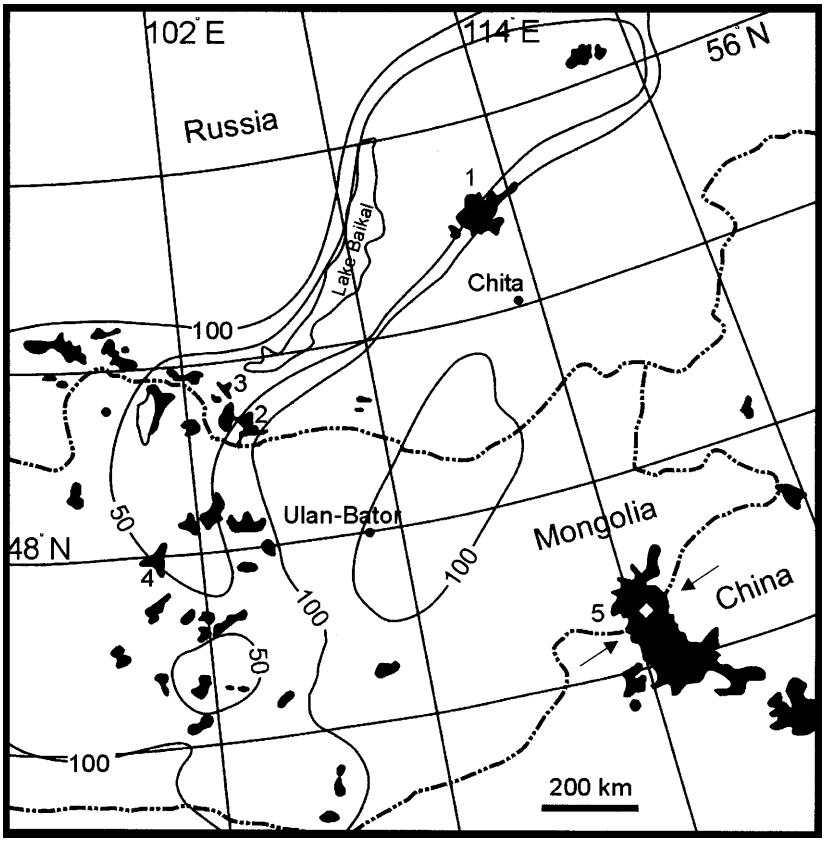

Fig. 1. Geographical sketch map of far-east Asia depicting the distribution of Cenozoic volcanic rocks (*Kononova* et al., 1993; *Zorin* et al., 1988). Main volcanic fields: (1) Vitim, (2) Dzida, (3) Bartoi, (4) Taryat, (5) Dariganga. White diamond (arrows) indicates the study area. Solid lines give the lithosphere thickness (in km)

titano-magnetite, olivine, mica, alkali feldspar and magnesian ilmenite, are known to occur at several Quaternary volcanoes and have been studied by different workers (*Kepezhinskas*, 1979; *Kononova* et al., 1986; *Genshaft* and *Saltykovsky*, 1990; *Wiechert* et al., 1997). Of these publications, only the last one contains high quality trace element and Sr-Nd, as well as O isotope data for a suite of peridotite xenoliths originating from the Achagyin-Dush volcanic centre, Dariganga, SE Mongolia. The contents and isotopic composition of sulphur in a larger collection of mantle xenoliths form the Dariganga volcanoes were studied earlier (*Ionov* et al., 1992).

Here we present major element analyses on bulk rock samples of another suite of Type I peridotite xenoliths and microprobe analyses of constituent phases. Instrumental neutron activation analysis (INAA) was also applied to determine trace element abundances in clinopyroxene, orthopyroxene and olivine separates and in whole-rock samples. Our suite of xenoliths originates mostly from the Volcano Achagyin-Dush (samples 2237a, 2237b, 2229); one sample (2132), was collected at an unnamed volcano situated in the vicinity of the Budun-Tologoi volcano.

Petrography

Xenoliths previously studied by *Wiechert* et al. (1997) were chosen in a manner to avoid effects of secondary alteration. In contrast, our suite of peridotite xenoliths was chosen to compare fresh with highly oxidised, black, altered samples. The rocks are composed of olivine, orthopyroxene, clinopyroxene and spinel. Hydrous minerals, such as amphibole and phlogopite, are absent.

Sample 2237a is a rounded nodule about 10×9 cm in size. It is a fresh, green, coarse-grained, protogranular, sheared spinel harzburgite (Fig. 2A). Olivine and orthopyroxene are present as large grains up to 8 mm in diameter. The large olivine grains are strongly kinked. Grain boundaries are mostly curviplanar. Generally, spinel is interstitial but a few blebs of spinel are included in olivines. Both orthopyroxene and clinopyroxene have exsolution lamellae. The mode, calculated from the bulk rock data (Table 1) and mineral compositions (Table 2), are as follows (in

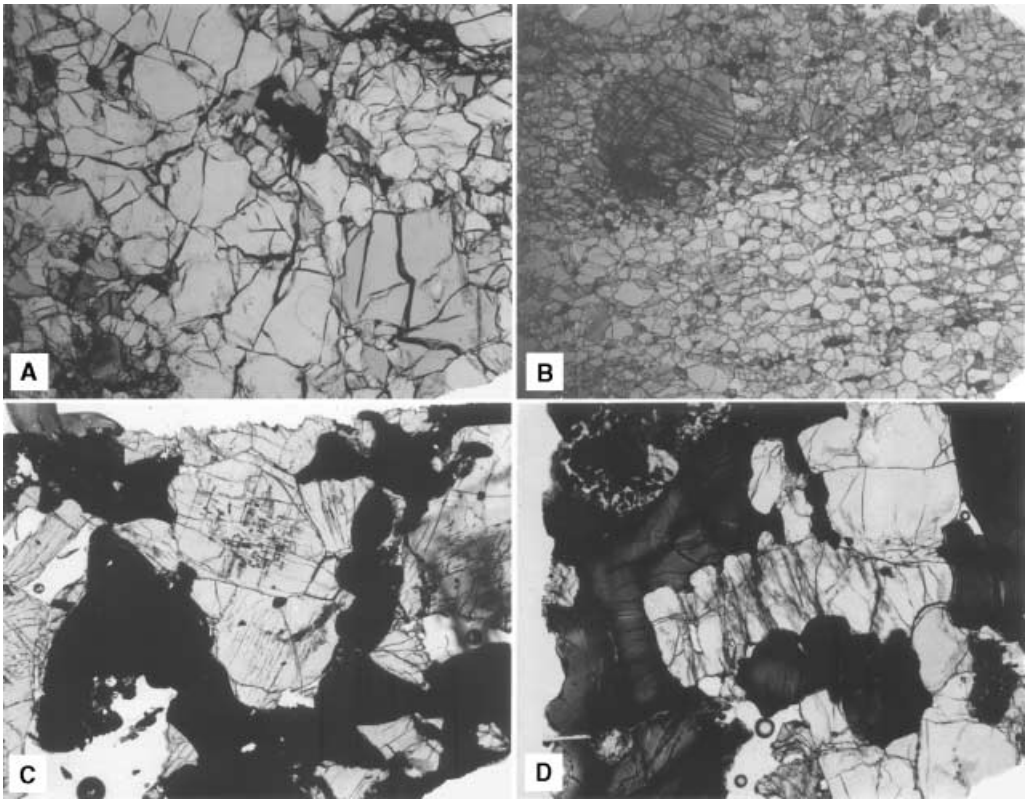

Fig. 2. Mongolian peridotites in thin section. **A** Harzburgite 2237a; large broken olivine (lower centre), orthopyroxene porphyroblast (lower right) and abundant small clinopyroxenes (left, dark grey); width of image is 17 mm. **B** Lherzolite 2132; re-crystallised with large clinopyroxene porphyroclasts (dark grey, upper left to right); width of image is 17 mm. **C** Lherzolite 2237b; olivine is black and pyroxenes have exsolution lamellae; width of image is 7 mm. **D** Lherzolite 2229; olivine (dark) is dark red in thin section and shows different degrees of reddening at grain margins, along cracks and in the interior. Note the palisade-type growth of orthopyroxene (centre) and melt pocket at upper left; width of image is 7 mm

Table 1. *Chemical composition of Dariganga peridotite xenoliths compared with primitive upper mantle composition*

Rock	GHB	GLH	BLH	BLH	PUM
Sample	2237a[#]	2132[&]	2237b[&]	2229[#]	
SiO_2	44.2	42.4	43.2	43.3	45.13
TiO_2	0.13	0.05	0.07	0.46	0.22
Al_2O_3	2.3	2.58	1.86	2.35	3.97
Cr_2O_3	0.44	0.39	0.40	0.31	0.46
Fe_2O_3	1.57	3.36	4.24	4.02	
FeO	6.72	7.18	5.75	7.73	7.82
MnO	0.13	0.15	0.14	0.11	0.13
MgO	41.5	39.7	41.5	39.0	38.3
NiO	0.26	0.26	0.29	0.26	0.27
CaO	0.97	2.67	1.46	1.51	3.50
Na_2O	0.22	0.37	0.42	0.49	0.33
K_2O	0.03	0.08	0.08	0.093	0.03
P_2O_5	0.08	< 0.04	< 0.04	< 0.04	
Total	98.55	98.54	98.37	99.90	100.16
mg no.	90.1	87.4	88.6	86.0	89.7

GHB green harzburgite; *GLH* green lherzolite; *BLH* black lherzolite; *PUM* primitive upper mantle (*Jagoutz* et al., 1979). # = wet chemical analysis, IGEM, Moscow; & = X-ray fluorescence analysis, IRM, Moscow

vol%): olivine 59.3, orthopyroxene 34.3, clinopyroxene 3.9, spinel 1.8. The calculation yielded a very high value for orthopyroxene and a relatively low one for clinopyroxene abundances. However, this is not supported by estimates of the modal composition, which suggest lower orthopyroxene and considerably higher clinopyroxene (8–10 vol%) contents. The cause of the discrepancy is probably the very low CaO content in the bulk rock analysis (Table 1).

Sample 2132 is an oval nodule about 6×3.5 cm in size. It is a light green spinel lherzolite rich in clinopyroxene (Fig. 2B). The mode is (in vol%): olivine 65.5, orthopyroxene 20, clinopyroxene 12.0, spinel 2.5. The sample is fine-grained, the average grain size is about 0.6 mm and the texture is equigranular tabular. The small neoblasts are inferred to have been in equilibrium with the stress field that caused the intensive recrystallization. A few much larger clinopyroxene grains, however, attest to an earlier coarser-grained texture, which probably existed before the final recrystallization. Relic large clinopyroxenes have thin exsolution lamellae of orthopyroxene, but the border zone of these grains is free of exsolution phenomena. Spinel is mostly interstitial and typically holly leaf-shaped, but there are smaller blebs of spinels that occasionally are included by different silicates. Neoblasts have straight planar boundaries, forming typical 120° triple junctions. Foliation and mineral layering is well developed, with clinopyroxene-rich layers being most abundant.

Sample 2237b is a black spinel lherzolite nodule about 6×9 cm in size (Fig. 2C). The black colour is due to oxide grain coatings and oxide inclusions, mainly in olivine (Figs. 3A–3C). Oxides replace olivine in a regular, oriented way, mimicking exsolution. The oxide-rich areas are oriented in at least three different

Table 2. *Electron microprobe analyses of minerals in peridotites from the Dariganga Plateau (in wt%)*

Rock	Harzburgite							Lherzolite						Lherzolite					
Sample	2237a							2132						2229					
Mineral	cpx	cpx	opx	opx	ol	sp	sp	cpx	cpx	opx	opx	ol	sp	cpx	cpx	opx	opx	ol	ol
SiO_2	53.0	52.8	55.5	55	39.9	0.10		51.7	52.7	55.4	56.4	40.3	0.06	48.9	46.8	52.2	52.2	40.0	42.4
TiO_2	0.37	0.40	0.06	0.07		0.08	0.26	0.68	0.57	0.11	0.12	0.02	0.04	1.73	2.73	0.58	0.59	0.02	0.03
Al_2O_3	5.6	6.0	3.1	4.0	0.04	49.4	46.5	6.3	6.4	3.9	4.0		58.7	7.5	8.4	5.2	5.3	0.03	0.06
Cr_2O_3	1.05	1.06	0.28	0.52		16.6	21.3	0.30	0.34	0.15	0.18	0.04	5.3	1.1	0.68	0.56	0.58	0.02	0.03
FeO	2.22	2.33	6.1	6.1	9.8	12.1	12.3	3.8	3.4	7.4	7.3	10.9	14.0	4.7	5.4	7.7	8.0	9.9	9.8
NiO	0.04	0.04	0.06	0.08	0.42	0.39		0.13	0.04	0.11	0.09	0.36	0.47			0.12	0.04	0.39	0.35
MnO	0.11	0.10	0.16	0.10	0.17	0.16		0.08	0.10	0.17	0.12	0.14	0.08	0.11	0.16	0.14	0.13	0.13	0.13
MgO	15.5	15.3	34.6	34.2	51.2	19.0	19.7	15.0	14.3	32.7	32.5	49.2	20.2	16.0	15.1	32.3	32.7	50.7	48.3
CaO	20.5	20.6	0.38	0.41	0.04	0.02		20.9	21.0	0.37	0.35	0.03		17.2	17.5	1.14	1.13	0.05	0.19
Na_2O	1.46	1.62	0.04	0.06				1.05	1.06	0.02				1.63	1.53	0.17	0.19		
Total	99.85	100.25	100.28	100.54	101.57	97.85	100.06	99.94	99.91	100.33	101.06	100.89	98.85	98.87	98.30	100.11	100.86	101.24	101.26
mg no.	92.6	92.1	91.0	90.9	90.3			87.6	88.2	88.8	88.8	89.0		85.9	83.3	88.2	87.9	90.1	89.8
cr no.	11.2	10.6	5.7	8.0		18.4	23.5	3.1	3.4	2.5	2.9		5.7	9.0	5.2	6.7	6.8		

Rock	Lherzolite					Lherzolite												
Sample	2229 cont.					2237b												
Mineral	ol (s)	ol (s)	ol (s)	sp	sp	cpx	cpx	cpx	opx	opx	ol	ol	ol (s)	ol (s)	ol (s)	ol (s)	sp	sp (rim)
SiO_2	38.0	40.0	36.3		0.25	52.3	52.9	52.9	56.1	55.5	39.8	40.2	41.7	41.7	37.9	38.3	0.03	0.09
TiO_2	0.09	0.04	0.06	1.08	1.41	0.28	0.2	0.23	0.09	0.04				0.02	0.02		0.13	0.29
Al_2O_3	1.02	0.06	0.42	42.9	41.7	4.1	4.3	4.1	2.98	2.96	0.05	0.04		0.02	0.04	0.05	41.7	14.6
Cr_2O_3	0.39	0.23	0.22	17.2	17.0	0.85	1.05	0.85	0.32	0.33		0.05	0.02				23.6	21.6
FeO	25.2	13.3	37.2	17.5	17.7	3.2	3.2	3.1	7.0	7.1	8.8	8.7	4.3	4.4	34.3	33.2	14.9	49.4
NiO	0.22	0.34	0.39		0.45			0.04	0.08	0.07	0.32	0.41	0.39	0.39	0.42	0.37	0.32	0.73
MnO	0.10	0.12	0.12	0.14	0.17	0.09	0.09	0.04	0.16	0.19	0.16	0.12	0.14	0.11	0.16	0.19	0.13	0.25
MgO	34.8	45.5	24.7	20.4	20.6	16.5	15.5	15.6	32.9	33.2	49.9	51.4	53.9	54.0	27.2	27.6	20.2	13.0
CaO	0.66	1.35	0.54		0.02	20.8	21.3	21.5	0.41	0.38	0.06	0.06	0.02	0.02	0.09	0.08		0.06
Na_2O	0.17	0.08	0.05		0.05	1.64	1.36	1.34	0.07	0.06								
Total	100.65	101.02	100.00	99.22	99.35	99.76	99.90	99.70	100.11	99.83	99.09	100.98	100.47	100.66	100.13	99.78	101.01	100.02
Mg no.	71.1	85.9	54.2			90.2	89.6	90.0	89.4	89.3	91.0	91.3	95.7	95.6	58.6	59.7		
Cr no.				21.2	21.5	12.2	14.1	12.2	6.7	7.0							27.5	49.8

cpx clinopyroxene, *opx* orthopyroxene, *ol* olivine, *sp* spinel, *s* secondary phase, Total Fe as FeO

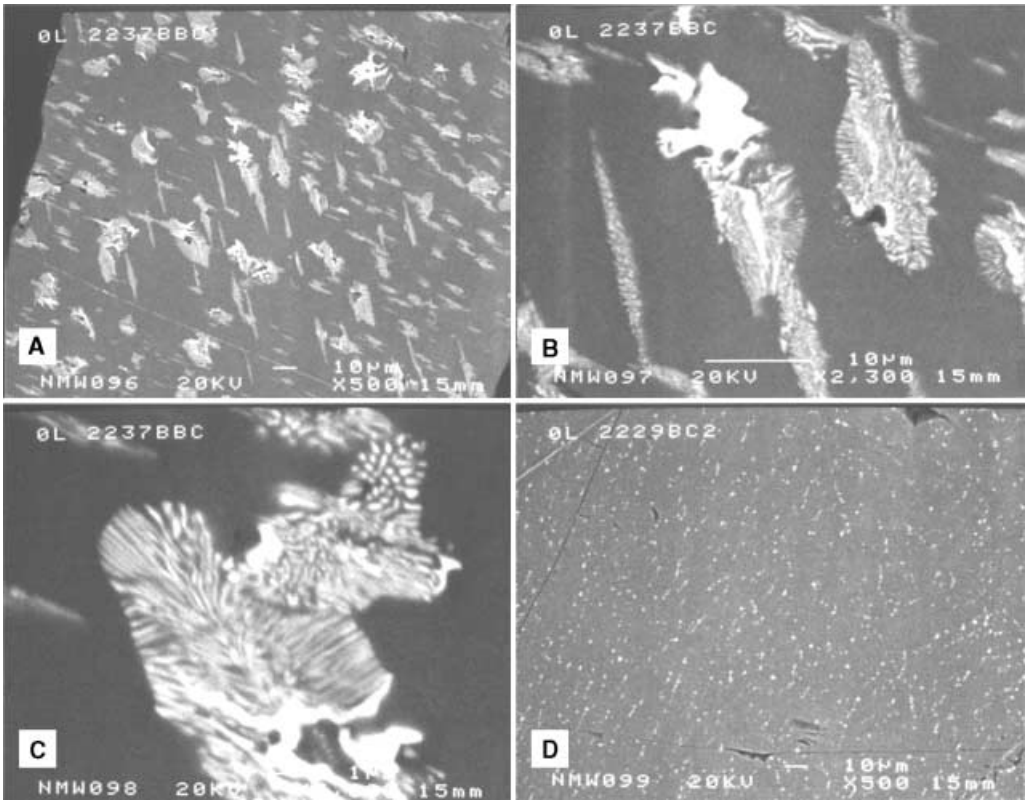

Fig. 3. Back-scattered electron scanning images of discoloured olivines. **A** Black olivines from black lherzolite 2237b. Iron oxide and Cr-rich spinel are distributed in an oriented manner in the olivine which is depleted in Fe (see Table 2). **B**, **C** Details from Fig. 3A showing symplectitic intergrowths of Fe oxide and olivine. **D** Black olivine (red in transmitted light) from lherzolite 2229. The oxide phase (presumably hematite) is very fine-grained and dispersed throughout the olivine

directions in the olivine. Close-ups reveal a symplectic intergrowth of olivine and an oxide phase (Fig. 3C). Pyroxenes are much less affected by this type of alteration than the olivine. The rock has an equilibrated medium grain-size texture. Spinel is mostly interstitial. The calculated mode is (in vol%): olivine 56, orthopyroxene 36, clinopyroxene 5.5, spinel 2.5.

Sample 2229 is a heavily altered, oxidised spinel lherzolite nodule about 5× 9 cm in size (Fig. 2D). Similar to sample 2237b, it is macroscopically black, but in thin section it appears red and does not show dendritic oxide patterns, but rather very fine-grained oxide segregations (Fig. 3D). All pyroxenes have a weak pleochroism from light green to light rose. This rock has a calculated mode of (in vol%): olivine 52, orthopyroxene 40, clinopyroxene 6, spinel 2.

Sample preparation and analytical procedures

About 30 to 100 g of bulk rock samples, depending on the material available, were crushed and powdered in an agate mortar. Whole-rock analyses were performed at

the Institute of Ore Deposits, Petrography, Mineralogy and Geochemistry (IGEM), Russian Academy of Sciences, Moscow. Major elements were analysed by classical wet-chemical methods and alkalis by flame photometry. Pressed powder pellets were used for the analysis of Rb, Sr, Ba, Zr and Y by X-ray fluorescence (XRF) utilising a VRA-20 instrument. Measurements were done against BCR-1 standard. Accuracy is estimated to be ±10–12 %. Samples for trace element analyses by INAA were taken from small rock specimens by breaking off ~1 g which were crushed and powdered in an automatic agate ball mill. Analyses were performed at the Institute of Geochemistry, University of Vienna. For details of instrumentation, procedures, and standards, as well as accuracy and precision of the data, see *Koeberl* (1993). Minerals were manually picked from rocks, rinsed in water and analysed following the same procedure.

Mineral compositions were determined with an ARL-SEMQ electron microprobe operated at 15 kV acceleration potential and 15 nA beam current. Analyses were made against natural and artificial mineral standards and subjected to standard correction procedures.

Results and discussion

Bulk rock major and minor element chemistry

Table 1 lists the major and minor element bulk rock analyses of the studied xenoliths and, for comparison, the composition of the primitive upper mantle (PUM) as estimated by *Jagoutz* et al. (1979). Major and minor element abundances in the Mongolian peridotites investigated are highly diverse, but, on average, correspond to those of ''depleted mantle'' (DM). Silica is moderately depleted (to 42.4 wt%) and MgO is slightly enriched (up to 41.5 wt%) as compared to PUM (45.1 wt% and 38.3 wt%, respectively), both indicating extraction of basaltic liquid. Aluminium and Ca have moderately depleted abundances suggesting extraction of moderate amounts of partial (basaltic) melts. The CaO/Al_2O_3 ratio varies from 0.42 to 1.03, i.e., from below to above the value in the PUM. Most CaO/Al_2O_3 ratios are below the PUM value suggesting fractionation by extraction of basaltic melt(s). This is also supported by a rough positive correlation between the CaO content and the CaO/Al_2O_3 ratio. However, there is no correlation between this ratio and the Al_2O_3 content. This fact contradicts a simple depletion by extraction of basaltic melt and indicates a disturbance by a third component, presumably a metasomatic enrichment. As CaO/Al_2O_3 ratios above the PUM value (0.88) can only be established by addition of CaO to the system, we can consider this as one of the mobile species during the metasomatic event(s).

Titanium is nominally less mobile than Ca and Al but has an abundance range from depleted ($TiO_2 = 0.05$ wt% in sample 2132) to enriched ($TiO_2 = 0.46$ wt% in sample 2229). The Al_2O_3/TiO_2 ratio ranges from well below (5.1) to well above (51.6) the PUM value (18.0). As there is no correlation with either Al or Ca, the variation of the Ti contents can also not be due to a simple melt extraction event but rather indicates a third component and an independent behaviour of Ti. As a high field strength element (HFSE), Ti can be mobilised either in a supercritical aqueous fluid or an alkali carbonatitic melt/fluid. Consequently, one of these agents likely percolated the Mongolian upper mantle.

Furthermore, Na and K are enriched over their primitive PUM abundances in black lherzolites 2237b and 2229 and also in green lherzolite 2132. Considering the moderate depletion of these rocks in Al and Ca, their enrichment in alkalis over the PUM abundances requires again a third component that was rich in these elements. An alkali metasomatism event is clearly indicated. As the alkali abundances are roughly anticorrelated with the mg-number, which ranges from approximately PUM to sub-PUM values, a concerted metasomatism involving alkalis and Fe is indicated. Consequently, the Fe contents are unusually high compared to the PUM composition, except for green harzburgite 2237a, which has an Fe content comparable to that of PUM. The Fe_2O_3/FeO ratio is unusually high in black lherzolites 2237b and 2229, suggesting that the blackening is intimately linked to oxidation. The bulk Fe content of the black samples (9.5 and 11.3 wt% Fe_{tot} as FeO, respectively) is significantly higher than that of PUM (8.2 wt% FeO). However, the green spinel lherzolite 2132 is also clearly enriched in Fe compared to PUM and is also fairly rich in Fe_2O_3. Only green harzburgite 2237a has a total Fe content similar to that of PUM. However, the content of Fe^{3+} is also disproportionally high in this sample ($\sim$20% of Fe_{tot}) – as it is in all other samples (up to $\sim$40% of Fe_{tot}). Discoloration of the rocks was clearly caused by oxidation, as indicated by the strongly increased Fe^{3+}/Fe^{2+} ratio, and by metasomatic addition of Fe.

The MnO contents are not elevated correspondingly to the Fe contents. They are on average slightly above PUM abundances and vary independently within narrow limits. Also, the Cr contents vary within tight limits but always are below that of PUM indicating moderate extraction of basaltic melt(s) (compare *Kurat* et al., 1980). No addition from the metasomatising agent is evident.

Major and minor element abundances testify to a complex history of the Mongolian xenoliths. Episodes of elemental extraction (by extraction of partial melts or by percolating fluids) and enrichments are indicated. Depletion in basaltic component is clearly suggested by low Si, Al, Ca, Ti and Cr contents as well as by commonly low CaO/Al_2O_3 ratios and by elevated MgO contents. The depletion event(s) was/were followed by metasomatic event(s) that lead to high contents of Fe and alkalis (all above PUM abundances) and occasionally high Ti content and a high CaO/Al_2O_3 ratio, indicating that the metasomatic agent was rich in these elements and Ca. All rocks have experienced severe oxidation which apparently was accompanying the metasomatic event and created high Fe_2O_3/FeO ratios. Of particular interest is the red lherzolite 2229, which appears to have been enriched in Fe, alkali elements and in Ti, indicating a type of metasomatic alteration that appears not to be very common in the uppermost mantle and that seems to be linked to the metasomatic growth of clinopyroxene porphyroblasts (e.g., see *Green* and *Wallace*, 1988; *Yaxley* et al., 1991; *Ionov* et al., 1993; *Varela* et al., 1999; *Kogarko* et al., 2001). An alkali-Ca-Fe carbonatitic melt/fluid is suggested by the features of this and all other rocks. The discoloration/oxidation event was accompanied by Fe metasomatism, however, the latter appears to have been taking place just before oxidation occurred.

Mineral chemistry

Electron microprobe analyses of the constituent phases reveal that the chemical compositions of primary minerals (Table 2) vary within the usual range

characteristic of continental UM peridotites (e.g., *Carter*, 1970; *Kuno* and *Aoki*, 1970; *Varne*, 1977; *Brown* et al., 1980; *Nickel* and *Green*, 1984; *Kurat* et al., 1980, 1993; *Embey-Isztin* et al., 1989). However, all xenoliths from Dariganga Plateau lack the usual perfect chemical equilibrium between rock-forming minerals. Also the green peridotites which do not reveal alteration exhibit subtle disequilibria indicating recent changes in mineral compositions.

Mineral phases in green lherzolite 2132 have compositions with low mg-numbers and extremely low cr-numbers ($100Cr/(Cr + Al)$, also in the spinel (Table 2). Surprisingly, the increase of mg-number is in the direction clinopyroxene $<$ orthopyroxene $<$ olivine, contrary to that usually observed in mantle peridotites (e.g., *Brown* et al., 1980; *Song* and *Frey*, 1989; *Embey-Isztin* et al., 1989). Minerals are apparently out of equilibrium with respect to the Fe-Mg distribution. Because diffusion of Fe^{2+} and Mg^{2+} is fastest in olivine, this phase should have adapted best to the latest conditions prevailing. Thus, the high mg-number of olivine compared to those of the pyroxenes could be due to extraction of Fe from the olivine, a process related to oxidation as it is well documented in the black peridotites (see below). Disequilibrium also exists among clinopyroxenes (variable Ti, Fe, Ni and Mg contents), a feature indicating compositional changes up to the time of delivery to the earth's surface.

Green harzburgite 2237a seems to be chemically equilibrated with respect to the Fe-Mg distribution among the major phases. Consequently, the order of increasing mg-number olivine (90.3) $<$ orthopyroxene (91) $<$ clinopyroxene (92.4) corresponds to the usual trend known from mantle harzburgites. Clinopyroxenes appear to be equilibrated but orthopyroxenes show subtle variations in their contents of Al, Cr and Mn. Spinels have variable cr-numbers (18–24) that correspond to UM harzburgite spinels. The cause for the non-equilibrium spinel composition is unknown but also indicates recent changes in either physical or – more likely – chemical conditions.

Oxidised lherzolite 2229 exhibits clear evidence for disequilibrium. The clinopyroxenes show varying compositions and are far too rich in Fe (mg# 83–86) to be in equilibrium with the coexisting olivine (mg# 90) and orthopyroxene (mg# 88), a case similar to but more strongly developed then that in green lherzolite 2132. Clinopyroxenes with such low mg-numbers are more characteristic of Type II than Type I xenoliths. Also, this clinopyroxene is rich in Ti and the orthopyroxene is very rich in Ti, Cr and Fe, outside the range of common UM orthopyroxenes. Both orthopyroxene and clinopyroxene appear to be the product of a metasomatic event that involved fluids rich in high-field strength elements (HFSE), Fe and alkalis. The event must have taken place under high pressure, as is indicated by the high Al contents of both pyroxenes. The apparent disequilibrium between clinopyroxene and orthopyroxene with respect to the Fe/Mg ratio could be due to a high Fe^{3+}/Fe^{2+} ratio in the clinopyroxene. In contrast, the composition of the olivine corresponds to that of a moderately depleted peridotite. The cr-number of the spinel, however, indicates a depleted, approximately harzburgitic original environment. In addition, relatively Fe-rich olivines (FeO up to 37 wt%, Table 2) are present in the rock and are inferred to be of secondary origin (see below).

Orthopyroxenes and clinopyroxenes in lherzolite 2237b have relatively low mg-numbers (89–90, Table 2). However, in the coexisting olivine this value is

higher (mg# up to 96) and shows an unusually large variability. Clearly, some of the olivines, especially those with mg-numbers >93 or <87, cannot be primary phases in Type I peridotites and the enrichment of the olivines in Fe must be of metasomatic origin. On the other hand, the depletion of olivines in Fe is likely to be due to oxidation of Fe^{2+} to Fe^{3+} and segregation of Fe oxides in the olivine, causing the blackening.

Clinopyroxenes in the black (2237b) and green (2237a) parts of the composite peridotite 2237 are similar in composition: they are rich in Al, Cr, Na and Ca. However, the Fe content is higher in the clinopyroxene of the black lherzolite 2237b as compared to that of the green harzburgite 2237a (by about 1 wt%), which suggests that a metasomatic event occurred and that Fe diffused into the clinopyroxene, but equilibration of pyroxene compositions was not achieved. Possibly, the event took place at too low a temperature to ensure equilibration by lattice diffusion and/or lasted for too short a time. In any case, it had to have taken place shortly before the sample was picked up and transported to the earth's surface.

In the black and red lherzolites (2229 and 2237b, respectively), olivines, pyroxenes and spinels occur that are clearly in disequilibrium with the co-existing primary phases and must have formed by secondary processes, such as melting, oxidation, or metasomatism. Oxidation is suggested by abundant oxide segregations in olivine (Fig. 3), melting by the presence of small melt pockets (Fig. 2D), and metasomatism by the enrichments of these minerals in Fe (and other elements). The Fe- and Ti-rich clinopyroxene of black lherzolite 2229 is probably the product of metasomatism and the more fayalite-rich olivines (mg# 85.9–54.2) could be the result of Fe metasomatism. In contrast, black lherzolite 2337b has both forsteritic and fayalitic disequilibrium olivines. The mg-number of the equilibrium olivine is about 91, whereas that of Fe-rich olivines is about 59 and that for forsteritic olivines is 96. Highly forsteritic olivines in spinel peridotite xenoliths may form by oxidation, whereby Fe is removed and concentrated in oxide phases, such as magnetite, hematite, and magnesioferrite (*Champness*, 1970; *Khisina* et al., 1995, 1998).

In summary, primary mineral compositions correspond to moderately depleted UM peridotites that have experienced metasomatic alterations by melts/fluids introducing alkalis, Ca, Al and Fe into these rocks. Equilibrium among phases was not achieved. Strong oxidation accompanied or followed the metasomatic event and created blackening of olivines by oxidation of Fe^{2+} to Fe^{3+} and precipitation of oxides in the olivines. This event also created Mg-rich olivine and caused Fe-Mg disequilibrium among phases not only in the black peridotites but also in green lherzolite 2132. Thus, minerals record extraction of basaltic melt, possibly several metasomatic events and a strong oxidation event, perhaps associated with the latest metasomatism.

Thermobarometry

Upper mantle xenoliths generally reflect ambient temperature and pressure conditions, provided that their mineral phases are homogeneous. However, persistent disequilibrium and unsuccessful re-equilibration of mineral compositions after entrapment in melts and during ascent to the surface have certainly influenced

Table 3. *Equilibration temperature and pressure estimates*

Sample	T °C (1)	T °C (2)	p kbar (3)
2237a	960	1000	24
2132	950	1000	21
2229	1150	1300	23
2237b	920	870	21

(1) *Wells* (1977); (2) *Brey* and *Köhler* (1990); (3) *Köhler* and *Brey* (1990)

the xenoliths of this study and, therefore, thermobarometric estimates should be used with caution. For example, the outstandingly high equilibration temperature estimate for the red lherzolite 2229 (1150/1300 °C, Table 3) is almost certainly wrong, as well as the overall high pressure values for spinel peridotites (> 20 kb). Considering the relatively low cr-numbers in the spinels, these pressure values are more consistent with the garnet peridotite stability field than with that of spinel-facies peridotites (*Webb* and *Wood*, 1986). This is not surprising, because the Ca-in-olivine barometer of *Köhler* and *Brey* (1990) is subject to great uncertainties (e.g., *O'Reilly* et al., 1997). Some of the peridotites (2237a and 2237b) yield relatively low temperatures of equilibration and the difference between the values obtained by the *Wells* (1977) and the *Brey* and *Köhler* (1990) geothermometers, respectively, is small (< 50 °C). It is assumed that these temperatures reflect a real equilibrium. Temperatures obtained with the *Wells* (1977) geothermometer vary between 920 °C and 960 °C in these rocks and are close to those obtained by *Wiechert* et al. (1997) from a suite of xenoliths of the Achagyin-Dush volcano (830–930 °C), who used the same equation.

Trace elements

Bulk rocks

Trace element abundances are summarised in Table 4 and the data are shown in chondrite-normalised diagrams (Figs. 4 and 5). There is some discrepancy between the bulk rock data obtained by wet chemical methods and X-ray fluorescence (Table 1) and those obtained by INAA (Table 4). In particular, the Fe and Cr values as obtained by the different methods are considerably different for most rocks. The worst cases are the harzburgite 2237a and lherzolite 2132 for the Fe contents and 2237a and 2229 for the Cr content. Some less dramatic differences are also present among the Ni and Na contents. Considering the sample preparation for the different bulk rock analyses, the wet chemical and X-ray fluorescence data clearly are the more representative bulk data. The INAA samples represented either single mineral grains or bulk samples of only about 100 mg. The very coarse-grained nature of the rocks and the irregular distribution of rare phases, such as spinel and clinopyroxene, and of alterations products likely led to non-representative sampling. In particular, the INAA sample of harzburgite 2237a had a deficit in olivine and spinel, that of lherzolite 2132 a deficit in olivine, that of lherzolite 2237b a deficit in spinel and that of lherzolite 2229 had a surplus in clinopyroxenes, all relative to the respective bulk. Unfortunately, quantification is not possible because of the inhomogeneous

Table 4. *Trace element contents of bulk xenoliths from Dariganga Plateau and their mineral separates (in ppm, unless indicated otherwise)*

Sample	2237a Green Harzb	2132 Green Lherz	2237b Black Lherz	2229 Black Lherz	2229BC Black opx	2229BC2 Black ol	2237aLG Green ol	2237aDG Green cpx	2237bBC Black ol
Na	1150	630	685	2440	1455	463	218	10120	115
Sc	9.01	8.66	7.96	12.4	9.84	2.43	1.7	61.2	1.57
Cr	760	2490	1945	3295	4665	872	60	7570	69
Mn	995	1165	1010	1060	1235	1520	1335	775	1455
Fe (wt%)	4.18	5.48	7.32	7.26	6.18	9.15	7.42	1.53	6.16
Co	87.4	95	131	122	74.2	173	161	19.9	128
Ni	1525	1950	2690	1928	815	3375	3180	< 600	2350
Zn	42	37	52	48					
Ga	1	1.2	1.5	3.5	5.2	2.6	0.15	< 1	0.69
As	0.047	0.071	0.19	0.042	0.19	0.092	0.036	0.79	0.075
La	0.65	0.33	0.77	0.42	0.048	0.034	1.75	5.34	0.38
Ce	2.32	0.46	1.48	1	0.45	0.31	4.4	10.8	2.2
Nd	0.59	0.27	0.7	0.78	0.55	0.26	2.6	5.8	1.3
Sm	0.136	0.077	0.164	0.4	0.14	0.11	0.12	1.37	0.04
Eu	0.043	0.026	0.055	0.16	0.071	0.048	0.043	0.37	0.027
Gd	0.13		0.16						
Tb	0.025	0.03	0.017	0.1	0.058	0.08	0.076	0.31	0.07
Dy	0.18	0.19	0.12	0.65	0.35	0.47	0.51	2.4	0.5
Ho	0.043	0.03	0.025						
Yb	0.17	0.14	0.066	0.46	0.34	0.32	0.33	1.95	0.3
Lu	0.03	0.032	0.01	0.071	0.05	0.05	0.05	0.27	0.05
Hf	0.062	0.035	0.16	0.67	0.042	0.16	< 0.2	0.28	0.1
W	0.026	0.036	0.048	0.05	0.08	0.04	0.017	< 0.05	0.028
Ir (ppb)	< 0.5	1	0.9	< 2	< 0.8	2	2	8	1
Au (ppb)	< 2	3	5	3					
Th	0.16	0.064	0.19	0.08	0.042	< 0.15	0.15	0.23	0.091
U	0.2			0.3	0.1				

Lherz lherzolite; *Harz* harzburgite; *ol* olivine; *opx* orthopyroxene; *cpx* clinopyroxene

composition of many phases. However, although the trace element data must also be affected by the sampling bias, dramatic distortions of the general abundance patterns can not be expected as most phases involved have low trace element abundances. The trace element abundances could be slightly shifted to high values for the same reason.

The lithophile elements in the bulk of the fresh, green peridotites (2237a and 2132) and the black peridotite 2237b show similar normalised abundance patterns (Figs. 4A and 5A). All have a roughly flat pattern for the moderately incompatible elements, which tend to be moderately depleted with respect to PUM. The highly incompatible elements are enriched over the less incompatible ones, except for Hf, whose abundance is low compared to those of La and Th, elements of similar incompatibility. All three rocks are slightly light rare earth (LREE)-enriched and have low abundances of heavy REE (HREE), a feature frequently observed in clinopyroxene-poor peridotites (e.g., *Frey* and *Prinz*, 1978; *Kurat* et al., 1980,

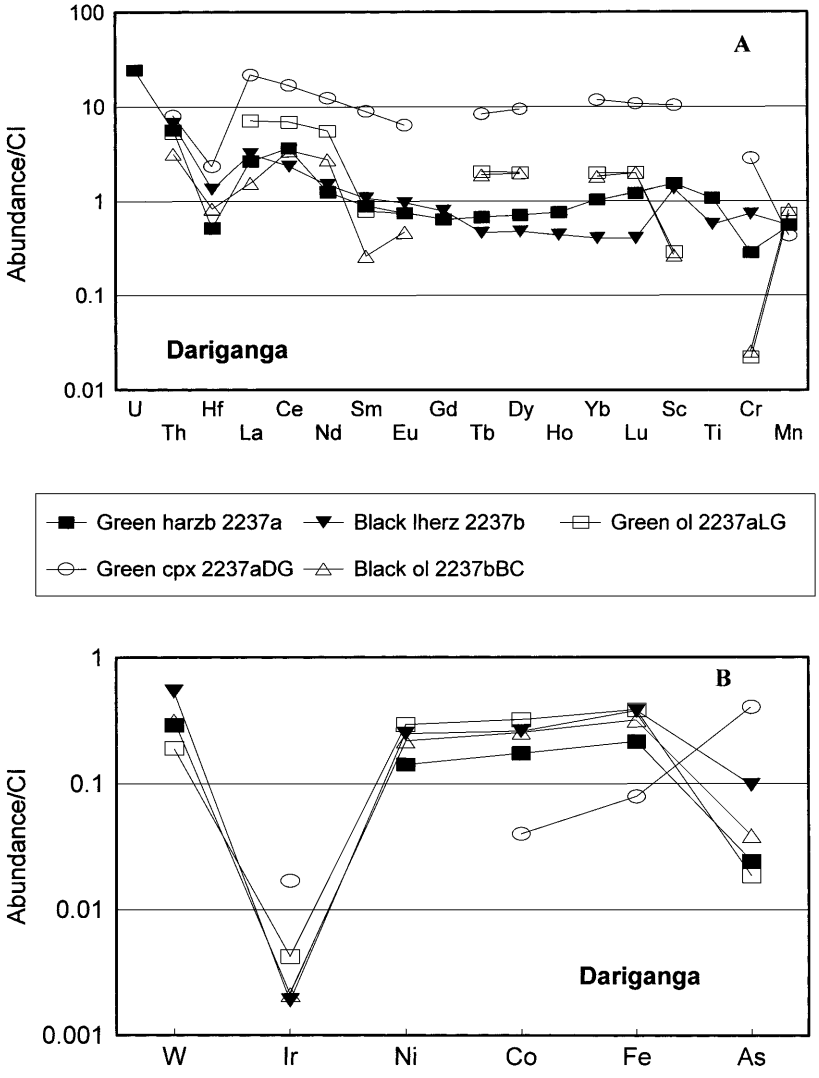

Fig. 4. Trace element abundances of bulk peridotites and mineral separates from composite sample 2237 normalised to abundances in the Orgueil CI chondrite (*Palme* and *Beer*, 1993). **A** lithophile elements; **B** siderophile elements

1993; *Stosch* and *Seck*, 1980; *Menzies*, 1983; *Wiechert* et al., 1997). The black lherzolite 2237b is poorer in HREE than the green peridotites by a factor of ∼0.5 which could indicate a more severe depletion event experienced by this rock as compared to the others.

Black lherzolite 2229 has trace element abundances similar to that of fertile UM. It shows pronounced positive anomalies in the Hf and U abundances with respect to geochemically similar elements, which are accompanied by a positive Ti anomaly.

Clearly, peridotites 2237a, 2237b and 2132 have experienced similar events that depleted them in incompatible elements. Peridotites 2132 and 2237b were somewhat more depleted than the others, as is indicated by their very low Hf and Ti, and HREE contents, respectively. An interesting case is provided by the

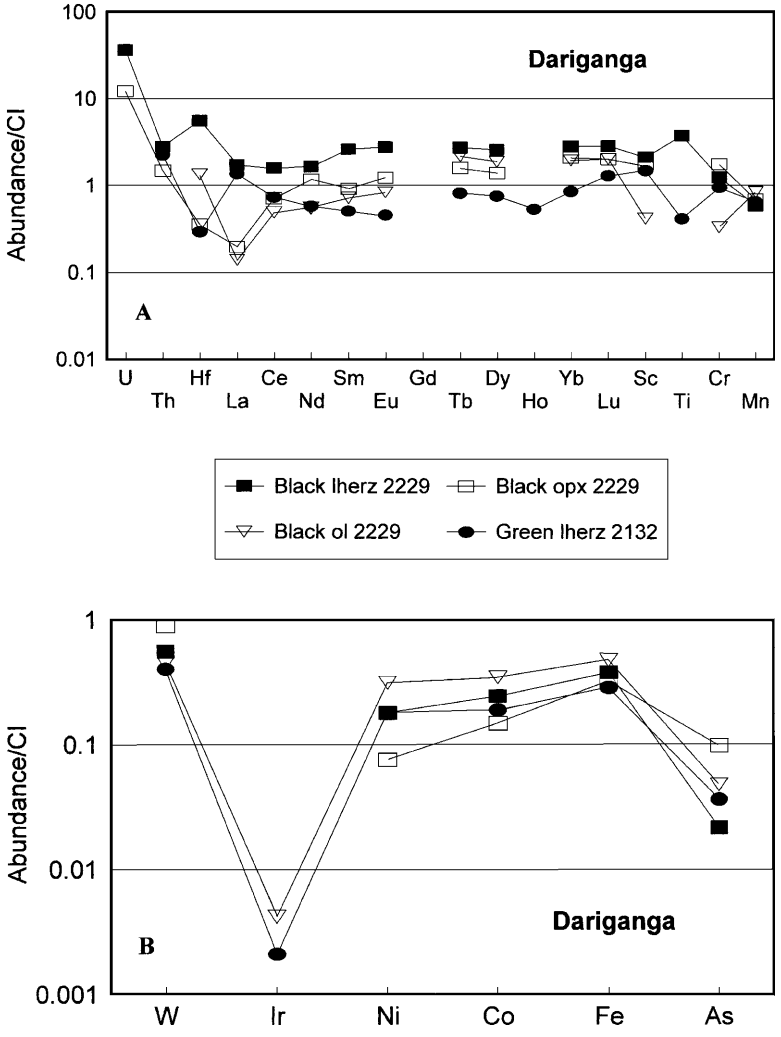

Fig. 5. Trace element abundances in bulk rock and mineral separates of black lherzolite 2229 and in bulk rock of green spinel lherzolite 2132 normalised to abundances in the Orgueil CI chondrite (*Palme* and *Beer*, 1993). **A** lithophile elements; **B** siderophile elements

composite peridotite sample 2237 of which the black part is clearly more strongly depleted in HREE than the green one. Part 2237b obviously has suffered more severe alterations than part 2237a which apparently was the less permeable rock that also preserved part of the original protogranular texture. We can speculate that tectonisation of part 2237b was the primary cause for the different behaviour of two portions of the same sample, similar to what has been reported from Zabargad Island peridotites (*Kurat* et al., 1993). All three rocks subsequently experienced a metasomatic event, which supplied mainly highly incompatible elements. The metasomatising fluid(s) carried incompatible elements with their abundances being proportional to their incompatibility, except for Hf. This could indicate the participation of CO_2 in the fluid phase, whereas the enrichment of U over Th (in harzburgite 2237a) could indicate participation of water.

The black lherzolite 2229 possibly has not experienced an extensive depletion event, but has also been subjected to an enrichment event caused by fluids rich in incompatible elements (inclusive HFSE). As this fluid delivered HFSEs (Ti, Hf, Th and U), it possibly contained alkali carbonate at a larger proportion compared to the fluids that metasomatised the other peridotites (e.g., compare *Green* and *Wallace*, 1988; *Yaxley* et al., 1991). These results are in general accordance with findings by *Wiechert* et al. (1997), who report low Hf contents to be associated with depleted and subsequently metasomatised peridotites from the same locality. However, they found in most cases – in contrast to our data – Th to be enriched over U, a feature in favour of a high CO_2 partial pressure in the fluid. Our data indicate that alkali carbonates were present as well as water, but its activity was low, as documented also by the lack of (OH)-bearing phases in Dariganga peridotitic xenoliths.

The siderophile elements (Figs. 4B and 5B) have bulk rock abundances similar to those in UM rocks. The bulk Ni, Co and Fe abundances vary probably due to the sampling problem as discussed above but some variation seems to be due to the (Fe) metasomatic event as the black peridotites tend to be richer in these elements compared to the green ones. The Ni/Co ratio is close to that of chondrites – similar to that of most UM rocks (Table 5). Iridium has low abundances in the bulk rocks, clearly below typical UM rocks (e.g., *Schmidt* et al., 2000), a feature for which we have no immediate explanation. Tungsten appears to be over-abundant, with the green peridotites at $\sim 2 \times$ UM and the altered peridotites at $\sim 3 \times$ UM abundances (e.g., *Newsom* et al., 1996). Considering the oxidising conditions in the PUM and those prevailing during the alteration of the peridotites, W was probably acting as a HFSE. If this was so, its enrichment should be correlated with similar enrichments in HFSE, like Th and also Ce. This is, however, not the case as the abundance of W is not correlated with that of these elements. As the variance of the abundances of both, Th and W, is limited, the W/Th ratio varies only between 0.16 (2237a) and 0.62 (2229) and overlaps with that of depleted UM (*Newsom* et al., 1996). The black peridotites are richer in W than the green ones. The enrichment of W could therefore be related to the Fe metasomatism and oxidation event but was independent of the HSFE enrichment event which therefore must belong to a different metasomatism episode.

Minerals

Trace element contents obtained by INAA on mineral separates from peridotites 2237a, 2237b and 2229 are fairly unusual. All olivine analyses show very high trace element abundances. The CI-normalised pattern of olivine is usually similar

Table 5. *Ni/Co ratios of bulk peridotites and olivine separates*

Sample	2237a Green Harzb	2132 Green Lherz	2237b Black Lherz	2229 Black Lherz	2229 Black Ol	2237a Green Ol	2237 Black Ol	CI Chondrite
Ni/Co	17.5	20.5	20.5	15.8	19.5	19.8	18.4	21.6^{+}

Harz harzburgite; *Lherz* lherzolite; *Ol* olivine. +: data *Palme* and *Beer* (1993)

to the pattern of the bulk rock. In the cases of green and black peridotites 2237a and 2237b, respectively, the olivine separates are richer in trace elements than the bulk rock. This is a clear indication that most of the trace elements reside in inclusions and/or at the surface of the olivine grains. As the olivines from the green and black peridotites (2237a and 2237b, respectively) have very similar trace element patterns (Fig. 4), these patterns must have been established prior to the blackening event. The co-existing clinopyroxene (from 2237a) has high ($\sim 10 \times$ CI) REE contents and a slightly LREE-enriched, otherwise flat pattern that follows the bulk pattern. This is additional evidence for the trace element pattern having been established prior to the blackening event because the clinopyroxene was not affected by this event, as is indicated by its chemical composition.

The overall REE abundances in the clinopyroxene separate from harzburgite 2237a are about one order of magnitude higher than in the corresponding whole-rock sample, indicating that most of the REE are hosted in clinopyroxene. Mass balance calculations based on a number of Achagyin-Dush xenoliths (*Wiechert* et al., 1997) show, however, that the clinopyroxenes account for only 10 to 60% of the LREE but 55 to 100% of the HREE of the bulk. This fraction is considerably smaller in LREE-enriched and higher in non-metasomatised peridotites. Consequently, a large part of LREE must reside in interstitial places, which becomes visible in the analyses of olivine separates, which were not acid-washed before analysis.

The clinopyroxenes separated from harzburgite 2237a show a negative Hf anomaly relative to Ce and Sm. However, no fractionation of Sc relative to Lu could be observed (Fig. 4). Fractionation of Sc, Hf, and Ta relative to REE was shown to be a characteristic feature of LREE-enriched clinopyroxenes from the Achagyin-Dush xenoliths, whereas no fractionation was observed in LREE-depleted clinopyroxenes (*Wiechert* et al., 1997).

The case for the black lherzolite 2229 is similar. The trace element abundance patterns for olivine and orthopyroxene follow that of the bulk rock, but at lower levels, except for La, which is depleted with respect to the other REE in the mineral separates (Fig. 5A). However, the black olivine has a strong positive Hf abundance anomaly that could indicate a correlation between oxide formation and HFSE-enrichment. On the other hand, orthopyroxene has elemental abundances increasing in the order La $<$ Hf $<$ Th $<$ U (from 0.2 to $\sim 10 \times$ CI). These elements are not likely to reside in the orthopyroxene, but could be concentrated in inclusions and/or at the grain surface. Therefore, the bulk trace element abundance pattern of this rock is likely to be dominated by inclusions in minerals and interstitial matter and has been established independent of the blackening event.

Siderophile element abundances in mineral separates show some peculiarities (Figs. 4B and 5B). Olivines have a pattern very similar to that of the bulk rocks, but at a slightly higher level. The clinopyroxene separated from green harzburgite 2237a is about ten-times enriched in Ir over the bulk rock. This enrichment is comparable in magnitude to the enrichments observed in an orthopyroxenite from Zabargad Island, but is much smaller than that found in a wehrlite from Zabargad Island (*Kurat* et al., 1993; *Schmidt* et al., 2000). The Ir-enrichment in clinopyroxene from harzburgite 2237a is accompanied by an enrichment of similar magnitude in As. Apparently, Ir and As were precipitated from the metasomatising

fluid that fed the growth of the clinopyroxene. Both elements possibly reside in fluid and/or sulphide inclusions.

Conclusions

The xenoliths from the Dariganga Plateau indicate that the upper mantle below SE Mongolia is not abnormally hot ($T_{equ} \sim 950\,^{\circ}C$ in spinel peridotite facies) and has a moderately depleted chemical composition. Previous studies in the nearby Taryat depression have shown the existence of more fertile upper mantle, where clinopyroxene-rich (>10 vol%) lherzolites are dominant and harzburgites are very rare (*Press* et al., 1986; *Stosch*, 1987). These data suggest that the mantle is more primitive below eastern Mongolia than in most other continental regions of the world. Also, the occurrence of garnet and garnet-spinel lherzolites in Mongolia and in Vitim, Trans-Baikal area (*Ionov* et al., 1992), is remarkable in continental alkali basalts and indicates the presence of an unusually thick continental lithosphere.

The overall history of the upper mantle underneath the Dariganga Plateau appears to have been complex. As in other localities, elemental depletions and enrichments processes testify to the activity of melts/fluids in the upper mantle. The rocks investigated have all been moderately depleted in incompatible elements and subsequently metasomatically enriched in alkalis, Fe, Ca, LREE, Th and U. Three of the four rocks show as a result of these processes moderately depleted Si, Cr, Ti, HREE and Hf, slightly enriched LREE and elevated Th and U abundances. However, none of them approaches the level of enrichment (up to $\sim 10 \times$ primitive UM) found in the Achagyin-Dush xenoliths by *Wiechert* et al. (1997). Only one of our samples belongs to the LREE-depleted group, which has been found to be common among the Achagyin-Dush xenoliths (*Wiechert* et al., 1997) and it displays only a weak depletion. Typically, all rocks have rather flat CI-normalised REE patterns.

The LREE-enriched peridotites and the clinopyroxene separate from one of them show negative Hf and Ti anomalies with respect to similarly incompatible elements and this corroborates the results of *Wiechert* et al. (1997) who concluded that the CO_2-rich micro-inclusions and negative anomalies of Nb, Hf, Zr, and Ti in primitive mantle-normalised trace element patterns of whole rocks and clinopyroxenes indicate that carbonate melts were responsible for the metasomatic enrichment. However, these carbonate melts must have been of an alkali-poor nature, or they were undersaturated in HFSE. Enrichment of U over Th in some of our samples seems also to indicate the presence of water in the fluid phase, however, the lack of (OH)-bearing minerals in the Dariganga xenoliths suggests a low activity of water in these fluids. A strong signal of carbonatitic melts/fluids seems to be present in one of our Dariganga peridotites. This rock was also enriched in Ti and Hf in a metasomatic event, indicating that beside water also some alkali carbonatitic melts/fluids were involved. The latest of these events probably took place shortly before entrapment of the rocks by the basalt that carried them to the earth's surface. Closely following this event is an independent oxidation event which led to precipitation of oxides in the olivine and blackening of the rocks. This blackening (and reddening) was accompanied by an addition of Fe that could have taken place anywhere between the upper mantle and the surface. No clear-cut

relationship between oxidation and metasomatism can be established. However, Fe metasomatism appears to have occurred after the oxidation took place as evidenced by Fe-rich olivines.

A composite sample consisting of a green harzburgite (2237a) and a black lherzolite (2237b) demonstrates that metasomatic processes in the upper mantle can be confined to rather restricted locations with sharp boundaries towards the wall rocks. It also demonstrates that rocks of different chemical and mineral chemical compositions can coexist in close contact for some (unknown) time. This sample also makes it likely that the oxidation event took place in situ in the upper mantle rather than during transport to the earth's surface. In the latter case the whole xenolith should have been affected, which clearly is not the case. Blackening, as the metasomatic events, was allowed to take place because of a better permeability in one part of the rock as compared to the other, likely the result of tectonisation.

Acknowledgements

This work was financially supported by the Austrian Research Fund (FWF) (projects P10670-GEO and Y58-GEO) and the Austrian Academy of Sciences. Constructive reviews by *B. G. J. Upton*, Edinburgh, and an anonymous reviewer helped to improve the manuscript.

References

Brey GP, Köhler TP (1990) Geothermobarometry in four phase lherzolites II. New thermometers, and practical assessment of existing thermometers. J Petrol 31: 1353–1378

Brown GM, Pinsent RH, Coisy P (1980) The petrology of spinel peridotite xenoliths from the Massif Central, France. Am J Sci 280A: 471–498

Carter JL (1970) Mineralogy and chemistry of the Earth's upper mantle based on the partial fusion-partial crystallisation model. Geol Soc Am Bull 81: 2021–34

Champness PE (1970) Nucleation and growth of iron oxides in olivines, $(Mg, Fe)_2SiO_4$. Min Mag 37: 790–800

Embey-Isztin A, Scharbert HG, Dietrich H, Poultidis H (1989) Petrology and geochemistry of peridotite xenoliths in alkali basalts from the Transdanubian Volcanic Region, West Hungary. J Petrol 30: 79–105

Frey FA, Prinz M (1978) Ultramafic inclusions from San Carlos, Arizona: petrologic and geochemical data bearing on their petrogenesis. Earth Planet Sci Lett 38: 129–76

Genshaft YS, Saltykovsky AY (1990) The catalogue of inclusions of deep-seated rocks and minerals in Mongolian basalts. Transact Joint Soviet-Mongolian Geolog Res Expedition, vol 46. Nauka, Moscow (in Russian)

Green DH, Wallace ME (1988) Mantle metasomatism by ephemeral carbonate melts. Nature 336: 459–462

Ionov DA, Hoefs J, Wedepohl KH, Wiechert U (1992) Content and isotopic composition of sulphur in ultramafic xenoliths from central Asia. Earth Planet Sci Lett 111: 269–286

Ionov DA, Dupuy C, O'Reilly SY, Kopylova MG, Genshaft YS (1993) Carbonated peridotite xenoliths from Spitsbergen: implications for trace element signature of mantle carbonate metasomatism. Earth Planet Sci Lett 119: 283–297

Jagoutz E, Palme H, Baddenhausen H, Blum K, Cendales M, Dreibus G, Spettel B, Lorenz V, Wänke H (1979) The abundance of major, minor and trace elements in the earth's

mantle as derived from primitive ultramafic nodules. Proc Lunar Planet Sci Conf 10th: 2031–2050

Kepezhinskas VV (1979) Cenozoic alkaline basaltoids of Mongolia and their deep-seated inclusions. Nauka, Moscow 311 pp (in Russian)

Khisina NR, Khramov DA, Kolosov MV, Kleschev AA, Taylor LA (1995) Formation of ferriolivine and magnesioferrite from Mg-Fe-olivine: reactions and kinetics of oxidation. Phys Chem Minerals 22: 241–250

Khisina NR, Khramov DA, Kleschev AA, Langer K (1998) Laihunitization as a mechanism of olivine oxidation. Eur J Mineral 10: 229–238

Koeberl C (1993) Instrumental neutron activation analysis of geochemical and cosmochemical samples: a fast and reliable method for small sample analysis. J Radioanalyt Nucl Chem 168: 47–60

Kogarko LN, Kurat G, Ntaflos T (2001) Carbonate metasomatism of the oceanic mantle beneath Fernando de Noronha island, Brazil. Contrib Mineral Petrol 140: 577–587

Köhler TP, Brey GP (1990) Calcium exchange between olivine and clinopyroxene calibrated as a geothermometer for natural peridotites from 2 to 60 kb with applications. Geochim Cosmochim Acta 54: 2375–2388

Kononova VA, Laputina IP, Pervov VA, Andreeva ED (1986) Find of a heterogeneous deep-seated inclusion in alkalic basaltic rocks of the Dariganga Plateau, Mongolian People's Republic. Dokl USSR Acad Sci 287(1): 105–108 (in Russian)

Kononova VA, Pervov VA, Drynkin VI, Kerzin AL, Andreeva ED (1987) Rare-earth and rare elements in the Cenozoic basic volcanites of Transbaikalia and Mongolia. Geochem Int 12: 32–46

Kononova VA, Ivanenko VV, Karpenko MI (1988) New data on K-Ar age of the Cenozoic continental basalts of the Baikal rift system. Dokl USSR Acad Sci 303(2): 454–458 (in Russian)

Kononova VA, Keller I, Pervov VA (1993) Continental basaltic volcanism and the geodynamic evolution of the Baikal-Mongolian Region. Petrology 1(2): 128–142

Kuno H, Aoki K (1970) Chemistry of ultramafic nodules and their bearing on the origin of basaltic magmas. Phys Earth Planet Int 3: 273–301

Kurat G, Palme H, Baddenhausen H, Hofmeister H, Palme Ch, Wänke H (1980) Geochemistry of ultramafic xenoliths from Kapfenstein, Austria: evidence for a variety of upper mantle processes. Geochim Cosmochim Acta 44: 45–60

Kurat G, Palme H, Embey-Isztin A, Touret J, Ntaflos T, Spettel B, Brandstätter F, Dreibus G, Prinz M (1993) Petrology and geochemistry of peridotites and associated vein rocks of Zabargad Island, Red Sea, Egypt. Mineral Petrol 48: 309–341

Menzies MA (1983) Mantle ultramafic xenoliths in alkaline magmas: evidence for mantle heterogeneity modified by magmatic activity. In: *Hawkesworth CJ, Norry MJ* (ed) Continental basalts and mantle xenoliths. Shiva Publishing, Nantwich, pp 92–110

Newsom HE, Sims KWW, Noll PD, Jaeger WL, Maehr SA, Beserra TB (1996) The depletion of tungsten in the bulk silicate earth: constraints on core formation. Geochim Cosmochim Acta 60: 1155–1169

Nickel KG, Green DH (1984) The nature of the uppermost mantle beneath Victoria, Australia as deduced from ultramafic xenoliths. In: *Kornprobst J* (ed) Kimberlites II. The mantle and crust-mantle relationships. Elsevier, Amsterdam, pp 161–178

O'Reilly SY, Chen D, Griffin WL, Ryan CG (1997) Minor elements in olivine from spinel lherzolite xenoliths: implications for thermobarometry. Min Mag 61: 257–269

Palme H, Beer H (1993) Abundances of the elements in the solar system. In: *Voigt HH* (ed) Astronomy and astrophysics, vol 3, subvol A. Instruments; methods; solar system. Springer, Berlin Heidelberg NewYork Tokyo, pp 196–221

Press S, Witt G, Seck HA, Ionov DA, Kovalenko VI (1986) Spinel peridotite xenoliths from the Taryat Depression, Mongolia. I. Major element chemistry and mineralogy of a primitive mantle xenolith suite. Geochim Cosmochim Acta 50: 2597–2599

Schmidt G, Palme H, Kratz K-L, Kurat G (2000) Are highly siderophile elements (PGE, Re and Au) fractionated in the upper mantle of the earth? New results on peridotites from Zabargad. Chem Geol 163: 167–188

Song Y, Frey FA (1989) Geochemistry of peridotite xenoliths in basalt from Hannuoba, Eastern China: implications for subcontinental mantle heterogeneity. Geochim Cosmochim Acta 53: 97–113

Stosch HG (l987) Constitution and evolution of subcontinental upper mantle and lower crust in areas of young volcanism: differences and similarities between the Eifel (F.R. Germany) and Taryat Depression (central Mongolia) as evidenced by peridotite and granulite xenoliths. Fortschr Mineral 65: 49–86

Stosch HG, Seck HA (1980) Geochemistry and mineralogy of two spinel peridotite suites from Dreiser Weiher, West Germany. Geochim Cosmochim Acta 44: 457–470

Tapponnier P, Molnár P (1979) Active faulting and Cenozoic tectonics of the Tien Shan, Mongolia and the Baikal regions. J Geophys Res 84: 3425–3459

Varela ME, Clocchiatti R, Kurat G, Schiano P (1999) Silicic glasses in hydrous and anhydrous mantle xenoliths from Western Victoria, Australia: at least two different sources. Chem Geol 153: 151–169

Varne R (1977) On the origin of spinel lherzolite inclusions in basaltic rocks from Tasmania and elsewhere. J Petrol 18: 1–23

Webb SAC, Wood BJ (1986) Spinel-pyroxene-garnet relationships and their dependence on Cr/Al ratio. Contrib Mineral Petrol 92: 471–480

Wells PRA (1977) Pyroxene thermometry in simple and complex systems. Contrib Mineral Petrol 62: 129–39

Wiechert U, Ionov DA, Wedepohl KH (1997) Spinel peridotite xenoliths from the Atsagin-Dush volcano, Dariganga lava plateau, Mongolia: a record of partial melting and cryptic metasomatism in the upper mantle. Contrib Mineral Petrol 126: 345–364

Yaxley GM, Crawford AJ, Green DH (1991) Evidence for carbonatite metasomatism in spinel peridotite xenoliths from Western Victoria, Australia. Earth Planet Sci Lett 107: 305–317

Zonenshain LP, Savostin LA (1981) Geodynamics of the Baikal rift zone and plate tectonics of Asia. Tectonophysics 76: 1–45

Zorin YuA (1981) The Baikal rift: an example of the intrusion of asthenospheric material into the lithosphere as the cause of disruption of lithospheric plates. Tectonophysics 73: 91–104

Zorin YuA, Balk TB, Novoselova MR, Turutanov EKh (1988) Lithosphere thickness under the Mongolia-Siberia mountain region and neighbouring territories. Izv Akad Nauk (Phyzika Zemli) 7: 33-42 (in Russian)

Authors' addresses: *V. A. Kononova* and *V. A. Pervov,* Institute of Geology of Ore Deposits, Petrography, Mineralogy, and Geochemistry (IGEM), Russian Academy of Sciences, Moscow, Russia, e-mail: victoria@igem.ru; *G. Kurat* and *F. Brandstätter,* Naturhistorisches Museum, Postfach 417, A-1014 Vienna, Austria; *A. Embey-Isztin*, Temeszettudomanyi Muzeum, POB 137, H-1431 Budapest, Hungary; *C. Koeberl,* Institut für Geochemie, Universität Wien, Althanstrasse 14, A-1090 Vienna, Austria